Journal of Human Genetics (2018) 63:699–706
https://doi.org/10.1038/s10038-018-0445-8

ARTICLE

Unfolded protein response is activated in Krabbe disease in a manner dependent on the mutation type

Kaori Irahara-Miyana[1] · Takanobu Otomo[1,2] · Hidehito Kondo[1] · Mohammad Arif Hossain[3,4] · Keiichi Ozono[1] · Norio Sakai[5]

Received: 10 October 2017 / Revised: 23 January 2018 / Accepted: 27 February 2018 / Published online: 3 April 2018

Abstract

Krabbe disease, one of the autosomal-recessive lysosomal storage disorders (LSDs), is caused by a deficiency of galactocerebrosidase (GALC) activity, resulting in the intracellular accumulation of psychosine, which is cytotoxic for neuronal cells. Genetically pathogenic mutations result in conformational changes in GALC and disrupt the lysosmal trafficking of cargos, which subsequently accumulate in the endoplasmic reticulum (ER). Recently, ER stress together with the activation of the unfolded protein response (UPR) has been suggested to play a key role in the pathogenesis of LSDs. In this study, we hence investigated whether the UPR is activated in Krabbe disease using COS-7 cells expressing pathogenic GALC mutants and skin fibroblasts (SFs) from Krabbe disease patients with various phenotypes, using a combination of semiquantitative and quantitative real-time polymerase chain reactions. We found that UPR activation in Krabbe disease depends on the mutations and cell types, and there is the possibility that multiple pathways, involving ER chaperones, inositol-requiring kinase 1, and protein kinase regulated by RNA-like ER kinase are activated by mutations associated with the infantile form. These results indicate that in Krabbe disease, each misfolded/unfolded protein evokes different UPR activation depending on the mutation, and that the activated pathways affect the phenotypes.

Introduction

Krabbe disease, also known as globoid cell leukodystrophy is one of the autosomal-recessive lysosomal storage disorders (LSDs) resulting from a deficiency of galactocerebrosidase (GALC) activity [1]. The GALC protein precursor (immature GALC) is an 80-kd protein comprising 669 amino acids, which is processed into the N-terminal fragment (50 kD) and C-terminal fragment (30 kD) [2–4], as mature GALC, presumably in the lysosome. We previously found that pathogenic missense mutations result in conformational changes in the GALC precursor, thereby disrupting its trafficking to lysosomes [5]. Such mutant proteins are localized in the endoplasmic reticulum (ER) or Golgi apparatus [6, 7]. where GALC hydrolyzes both galactocerebroside and psychosine (galactosylsphingosine), which are specifically cytotoxic to oligodendrocytes and Schwann cells, respectively [8, 9]. Therefore, Krabbe disease is caused by demyelination in both the central and peripheral nervous systems, with the accumulation of mainly psychosine [10]. Phenotype–genotype correlations can be seen with some mutations, such as c.635–646delinsCTC, p.P302A, p. D528N, and p.T652P for infantile onset and p.G270D and p.L618S for adult onset Krabbe disease. These findings indicate that Krabbe disease may involve the accumulation of GALC proteins with different conformational changes depending on the mutation, and in various organelles, in addition to the cytotoxicity of

Electronic supplementary material The online version of this article (https://doi.org/10.1038/s10038-018-0445-8) contains supplementary material, which is available to authorized users.

✉ Norio Sakai
norio@ped.med.osaka-u.ac.jp

[1] Department of Pediatrics, Osaka University Graduate School of Medicine, Osaka, Japan

[2] Department of Pathophysiology and Metabolism, Kawasaki Medical School, Okayama, Japan

[3] Advanced Clinical Research Center, Institute of Neurological Disorders, Shin-Yurigaoka General Hospital, Kanagawa, Japan

[4] Department of Gene Therapy, Institute for DNA Medicine, The Jikei University School of Medicine, Tokyo, Japan

[5] Department of Health Science, Child Healthcare and Genetic Science, Osaka University Graduate School of Medicine, Osaka, Japan

psychosine. Proteins that mature with folding or intra/intermolecular disulfide bond formation in the ER, are subsequently transported to their destinations. However, if proteins fail to adopt their proper conformation, they accumulate in the ER lumen and disrupt ER homeostasis, which leads to a condition referred to as ER stress. To maintain homeostasis in the ER, a quality control system exists to determine whether newly synthesized proteins are folded properly. If abnormal proteins are detected within the ER, cells activate the unfolded protein response (UPR) via three ER transmembrane proteins, namely, activating transcription factor 6 (ATF6), inositol-requiring kinase 1 (IRE1), and protein kinase regulated by RNA-like ER kinase (PERK) the main sensors of the UPR in eukaryotes [11].

In the steady-state, IRE1 and PERK are inactivated by their binding with 78 kDa glucose-regulated protein (GRP78) (also known as Binding immunoglobulin protein), which acts as an ER chaperone. The accumulation of unfolded/misfolded proteins evokes GRP78 dissociation from these proteins, followed by the subsequent activation of the three receptors, which transmit downstream signals. ATF6 translocates to the Golgi upon conditions of ER stress, where it is cleaved by site 1 and site 2 proteases to release the soluble N-terminal fragment. Translocation of this fragment to the nucleus induces the expression of a spectrum of UPR mediators, including ER chaperones, as typified by GRP78, and enhances the proper folding of proteins in the ER. IRE1 dimerizes after dissociation of GRP78 followed by autophosphorylation of the kinase domain and activation of the RNase domain. The activated RNase domain of IRE1 catalyzes the removal of a small intron from the mRNA of the gene encoding X-box-binding protein (XBP1), resulting in the production of spliced XBP1 proteins (XBP1-s), which indicates the indirect activation of the IRE1 pathway [12, 13] and subsequently inducing apoptosis. PERK-induced phosphorylation of eukaryotic initiation factor 2α (eIF2α) leads to translational attenuation [14, 15]. PERK also dimerizes or oligomerizes after the dissociation of GRP78 followed by autophosphorylation of the kinase domain. Activated PERK specifically phosphorylates eIF2α, which inhibits DNA transcription, resulting in a reduced level of new protein synthesis in the ER. C/EBP (CCAAT/enhancer binding protein) homologous protein (CHOP), which is a common downstream factor of the PERK-ATF4 and ATF6 pathway, activates proteins, such as DNA damage-inducible gene 34 and Bcl-2 interacting mediator of cell death. In addition to these pathways, ER chaperones, such as GRP78 or Homocysteine-responsive endoplasmic reticulum-resident ubiquitin-like domain member 1 (HERPUD1), which bind unfolded/misfolded proteins or retrotranslocate them to the cytoplasm, also play a role in the UPR.

In LSDs, including GM1-gangliosidosis, neural ceroid lipofuscinosis, Tay-Sachs disease, and Gaucher disease, the UPR pathway is thought to play a role [16–20]. However, the role of UPR in Krabbe disease has not been investigated previously. Therefore, in the present study, we used COS-7 cells expressing pathogenic mutations in which phenotype–genotype correlations are apparent, and used cultured SFs derived from patients with Krabbe disease, to investigate whether UPR activation occurs in Krabbe disease.

Materials and methods

Cloning and construction of expression vectors of human GALC

Wild-type human GALC cDNA, containing a fragment from 19-bp upstream from the first ATG translation initiation site [21] to the AseI site (178-bp downstream from the stop codon) was constructed in a pSVL vector (GE healthcare, Amersham, UK), and six mutations including c.635–646delinsCTC, p.G270D, p.P302A, p.D528N, p.L618S, and p.T652P were introduced by polymerase chain reaction (PCR), and the sequence of all constructs were confirmed by DNA sequencing, as previously described [5].

Transfection and cell culture

COS-7 cells were prepared on the day prior to transfection. Briefly, both 2.7 μL of TransFectin™ Lipid Reagent (Bio-Rad Laboratories K.K., Tokyo, Japan) and 0.7 μg of plasmids, including the empty vector (mock), wild-type GALC cDNA, and GALC mutant constructs were diluted using Dulbecco's Modified Eagle Medium (Life Technologies Co., Carlsbad, CA) with 10% fetal bovine serum (referred to as regular medium) to a final volume of 200 μL according to the manufacturer's instructions, and then mixed together following incubation at room temperature for 20 min. For the cotransfection of two types of GALC mutant constructs, 0.35 μg of each plasmid was added. Then, $0.2–0.25 \times 10^6$ cells were added to the incubated solution to a final volume of 1000 μL with regular medium to be seeded in 12-well plates (Greiner Bio-one, Kremsmünster, Austria). Transfection reactions were performed for 48 h in a 5% CO_2 incubator at 37 °C, and finally cells were collected for RNA isolation.

Patients

This study included four Japanese patients. Their diagnosis was based on clinical symptoms, neurological findings,

Table 1 Expression of each UPR gene in patient SFs, and patient phenotypes

	c.635–646delinsCTC/ c.635–646delinsCTC	c.635–646delinsCTC /T652P	P302A/ L618S	L618S/ L618S
Phenotype (onset)	Infantile (3 months)	Infantile (6 months)	Juvenile (3 years)	Adult (45 years)
CHOP	**	****	****	**
ATF6	*	*	*	ND
GRP78	ND	N.D.	ND	△*
HERPUD1	**	**	**	ND
XBP1s	ND	*	*	ND

ND no significant difference

* Significant difference (increase) $p < 0.05$

** Significant difference (increase) $p < 0.01$

**** Significant difference (increase) $p < 0.001$

△* Significant difference (decrease) $p < 0.05$

laboratory confirmation of low GALC activity in lymphocytes, and pathological mutations. The mutations found in three of the patients had been identified previously [5], and one was a newly confirmed mutation (Table 1). GALC mutations in the present report are described following the nomenclature reported previously [22, 23].

Genomic DNA analysis by direct sequencing

DNA was prepared by standard methods from patient lymphocytes. PCR reactions and direct sequencing were conducted as previously described [23].

Patient SFs

SFs were established from all four patients. The normal human dermal fibroblast cell line was purchased from Gibco (Thermo Fisher Scientific, MA, USA). SFs were cultured in regular medium containing 1% antibiotic-antimycotic solution in a 5% CO_2 incubator at 37 °C for 48 h prior to cDNA extraction. The number of passages of all SFs used was <10 times.

Measurement of GALC activity

Enzyme activity was measured using 6-hexadecanoylamino-4-methylumbelliferyl-β-D-galactopyranoside (HM-gal) (Slater and Frit Ltd, Norwich, UK) as an artificial fluorescence substrate following the Wiederschain protocol [24].. Briefly, collected cells were sonicated and incubated with the substrate in citrate-phosphate (CP) buffer (pH 4.2) at 37 °C for 4 h and fluorescence (excitation at 385 nm/emission at 450 nm) was measured using a microplate reader. Enzyme activity was calculated as nmol/h/mg protein.

RNA extraction and DNA preparation

Total RNA was extracted from cells using NucleoSpin® RNA (Takara, Kusatsu, Japan) and subsequently cDNA was extracted using ReverTra Ace qPCR RT Master Mix with gDNA Remover (TOYOBO, Osaka, Japan) according to the manufacturer's instructions. This kit contained a DNase step. cDNA products were frozen at −20 °C.

Real-time reverse transcription-PCR (RT–PCR)

Real-time quantitative RT–PCR (qPCR) was performed using SYBR Green PCR Master Mix (TOYOBO) and ABI PRISM 7900HT with cDNA (equivalent to 30 ng of total RNA for the analysis of *CHOP*, *ATF6*, *GRP78*, and *HERPUD1* and 10 ng for the analysis of *GAPDH*. The primer concentration was 0.45 nM in a reaction volume of 15 µL. Each reaction was performed in triplicate or twice in triplicate. The thermal cycling parameters were as follows: 95 °C for 1 min, 40 cycles of 95 °C for 15 s and 60 °C for 45 s, and a final cycle at 95 °C for 15 s, 60 °C for 15 s and 95 °C for 15 s. Relative expression of mRNA for the target genes was performed by the comparative CT method using the *GAPDH* gene as a control. Data are presented as means ± SE. *P*-values were calculated using analysis of variance and a *p*-value of less than 0.05 was considered to indicate a statistically significant difference between two groups. Sense and antisense primer sequences for RT–PCR amplification are shown in Supplementary Table.

XBP-1 splicing assay

After first-strand cDNA synthesis, PCR was carried out using KOD Plus (TOYOBO) for 94 °C (two min), 35 cycles at 98 °C (10 s), 48 °C (30 s), and 68 °C (30 s) for *XBP-1* and 94 °C (2 min), 30 cycles at 98 °C (10 s), 55 °C (30 s), and

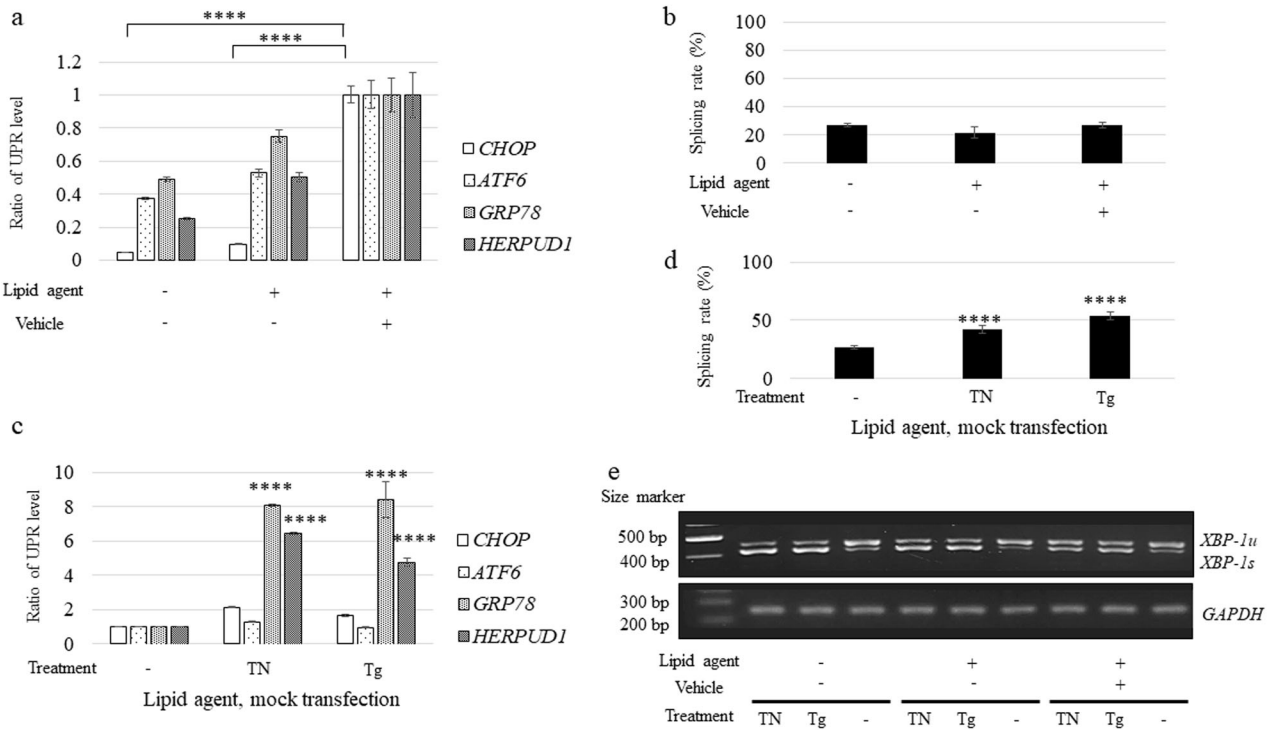

Fig. 1 Effect of the expression of each UPR protein in COS-7 cells. **a** mRNA levels of *CHOP*, *ATF6*, *GRP78*, and *HERPUD1* were compared upon treatment with a lipid agent and mock transfection. **b** Splicing rate of *XBP-1* under each transfection condition was calculated by the ratio of the band intensities of *XBP-1s* to *XBP-1u* (*XBP-1*s / [*XBP-1s* + *XBP-1u*]). The DNA templates used were the same as those used in **a**. **c** mRNA levels of *CHOP*, *ATF6*, *GRP78*, and *HERPUD1* with TN or Tg treatment were compared to no treatment with transfection. (**d**) Splicing rate of XBP-1 under each treatment condition was calculated by the ratio of the band intensities of *XBP-1s*/[*XBP-1s* + *XBP-1u*] (**e**) Electrophoresis of *XBP-1u and XBP-1s* under different treatment conditions of lipid agents, vehicle, and TN/Tg. Splicing ratios were calculated using this figure. Data are shown as the mean ± SE ($n = 3$) *$p < 0.05$, **$p < 0.01$, ***$p < 0.005$, ****$p < 0.001$ vs. no lipid reagent, no vehicle, or no treatment group. TN tunicamycin, Tg thapsigargin, NC negative control

68 °C (16 s) for *GAPDH* containing 20 ng of each cDNA obtained from both COS-7 cells and SFs. PCR reactions were subjected to electrophoresis through a 2% agarose gel to distinguish the unspliced (*XBP-1u*, 473 bp) from the spliced band (*XBP-1s*, 447 bp). Splicing rate was calculated by the ratio of *XBP-1s* to *XBP-1u* band intensities using Image Lab software (Bio-Rad Laboratories K.K., Tokyo, Japan). Sense and antisense primers used were 5′-ccttgtagttgagaaccagg−3′ and 5′-ggggcttggtatatatgtgg−3′.

Induction of UPR compounds in transfected COS-7 cells by tunicamycin and thapsigargin treatment

Cytotoxicity assays were performed using tunicamycin (TN) and thapsigargin (Tg). In each experiment, COS-7 cells transfected with empty vector (mock), wild-type GALC cDNA, and GALC mutant constructs (0.2–0.25 × 10^6 cells/well/1000 µL regular medium) were plated at time zero in 12-well plates. After 48 h, 1 µL of TN or Tg dissolved in deionized-distilled H_2O (dd H_2O) was added to different wells at final concentrations of 1 µg/mL for TN and 1 µM for Tg. In all the experiments, 1 µL ddH_2O was added to the control wells. Cells were then incubated for 6 h in a humidified atmosphere containing 5% CO_2 at 37 °C. After this incubation, cells were collected for RNA isolation and subsequent RT–PCR analysis.

Results

GALC enzyme activities in COS-7 cells and patient SFs

We prepared lysates of COS-7 cells transfected with each expression construct and of patient SFs, and measured their GALC enzyme activities. GALC enzyme activities of cells expressing GALC with infantile onset mutations were similar to mock-transfected cells, whereas cells expressing GALC with adult onset mutations showed higher enzyme activity, and cells expressing the G270D mutant showed almost normal enzyme activity (Fig. 2a). On the other hand, unlike COS-7 cells, no apparent association was observed between enzyme activity and phenotype in patient SFs (Fig. 3a).

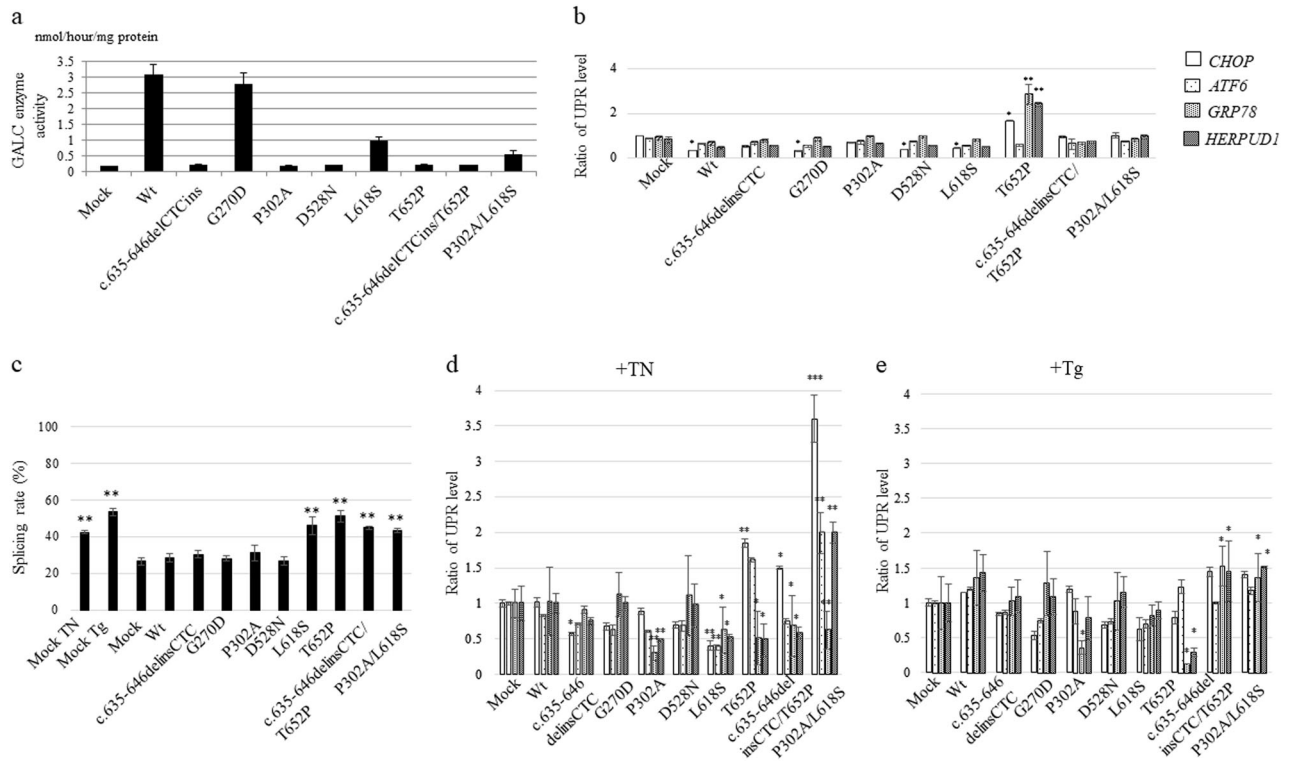

Fig. 2 **a** GALC enzyme activities measured using HM-gal substrate in COS-7 cells expressing wild-type or mutant GALC. **b–e** Effect of the expression of GALC mutants on the levels of various *UPR* genes in COS-7 cells. (mock, $n = 6$; other mutations, $n = 3$) (**b**) mRNA levels of *CHOP*, *ATF6*, *GRP78*, and *HERPUD1* upon the expression of each mutant were calculated as a ratio to mock transfection, which was set as 1 (**c**) Splicing rate of *XBP-1* upon the expression of each mutant was calculated by the ratio of the band intensities of *XBP-1s* to *XBP-1u*, as in Fig. 1d. **d**, **e** mRNA levels of *CHOP*, *ATF6*, *GRP78*, and *HERPUD1* with TN (**c**) or Tg (**d**) treatment were compared with mock transfection. The mRNA level was calculated as a ratio with the mock transfection with treatment group considered as 1. $*p < 0.05$, $**p < 0.01$, and $***p < 0.005$ vs. the mock transfection group (**a**, **b**) or mock transfection with treatment (**c**, **d**)

Effect of transfection procedures on the expression of UPR target genes in COS-7 cells

As some transfection procedures (e.g., sonoporation) induce the UPR [25], we analyzed the effects of lipid transfection reagents on the expression of UPR target genes. No UPR target genes were increased or decreased by the transfection reagent without vector compared with no treatment; however, *CHOP*, *ATF6*, and *HERPUD1* were activated by transfection reagents containing the mock vector. Both *ATF6* mRNA and the level of *XBP-1* mRNA splicing did not show any changes in all conditions. (Fig. 1a, b, e).

Effect of TN and Tg on the expression of UPR target genes in COS-7 cells

TN and Tg, which are UPR-inducing compounds, inhibit protein glycosylation in the ER and ER calcium ATPase activity, respectively. These UPR compounds induced a significant increase in the mRNA levels of *GRP78* and *HERPUD1*, *XBP-1* mRNA splicing levels, as well as a mild increase in *CHOP* mRNA compared with no treatment in mock-transfected COS-7 cells (Fig. 1c, d, e).

Effect of mutant GALC expression on UPR target gene expression

Expression of the T652P GALC mutant showed a significant increase in the mRNA levels of *CHOP*, *GRP78*, and *HERPUD1*, as well as the level of *XBP-1* mRNA splicing (Fig. 2b, c, Table 2), whereas the expression of L618S showed a significant decrease in the mRNA level of *CHOP* as well as the level of *XBP-1* mRNA splicing. The expression of c.635–646delinsCTC/T652P and P302A/L618S showed a significant increase in *XBP-1* mRNA splicing (Fig. 2c). Wild G270D, and D528N inhibited the mRNA levels of *CHOP*.

Effect of tunicamycin and thapsigargin on mutant GALC transfection

Under TN treatment, compared with mock transfection, P302A/L618S activated the response of *CHOP*, *ATF6*, and

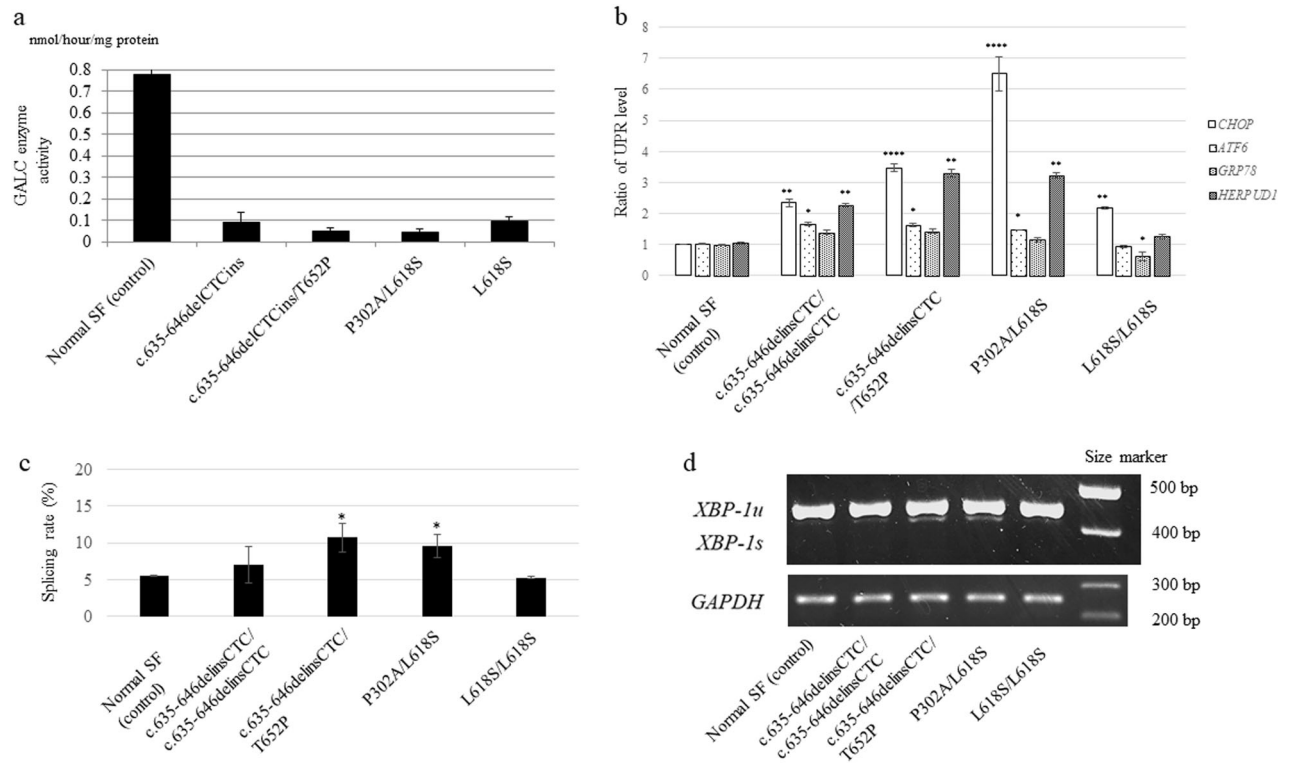

Fig. 3 **a** GALC enzyme activities measured using HM-gal substrate in patient SFs. **b–d** Levels of UPR genes in patient SFs. **b** mRNA levels of *CHOP*, *ATF6*, *GRP78*, and *HERPUD1* were compared with normal SFs as a standard. **c** Splicing rate of *XBP-1* in the SFs of each patient calculated in Fig. 1d. Statistical analysis was calculated using normal SFs as a standard. The same DNA templates as in Fig. 3b were used. **d** Electrophoresis of *XBP-1u* and *XBP-1s*. Splicing ratios were calculated using this figure. ($n = 3$) $^{*}p < 0.05$, $^{**}p < 0.01$, and $^{****}p < 0.001$ vs. normal SF

HERPUD1, and inhibited the response of *GRP78*, whereas T652P and c.635–646delinsCTC/T652P activated the response of *CHOP* and inhibited the response of *GRP78* and *HERPUD1*, and P302A inhibited the response of *GRP78* and *HERPUD1*, and L618S inhibited all of these four UPR factors (Fig. 2d). On the other hand, under Tg treatment, c.635–646delinsCTC/T652P and P302A/L618S activated the response of *GRP78* and *HERPUD1*, T652P inhibited the response of *GRP78* and *HERPUD1*, and P302A inhibited the response of *GRP78* but not *HERPUD1*, which was different from TN treatment (Fig. 2e). These changes were all statistically significant, although most of them changed by less than two-fold.

UPR levels in patient SFs

c.635–646delinsCTC/c.635–646delinsCTC showed an increase in the mRNA levels of *CHOP*, *ATF6*, and *HERPUD1*, and c.635–646delinsCTC/T652P and P302A/L618S showed an increase in the mRNA levels of *CHOP*, *ATF6*, and *HERPUD1*, as well as *XBP-1 s*plicing, and L618S/L618S showed an increase in *CHOP* and the inhibition of *GRP78* (Fig. 3b, c, d, Table 1). An increasing ratio of *ATF6* showed statistical significance but was not obviously different compared with *CHOP* and *HERPUD1*.

Discussion

The major finding of the current study is that UPR activation in Krabbe disease has selectivity depending on the mutation.

In COS-7 cells, T652P activated multiple UPR factors, such as *CHOP*, *GRP78*, *HERPUD1*, and *XBP1s*. This indicates activation of the ER chaperones and each downstream pathway of IRE1 and PERK. The PERK pathway works as a controller of DNA transcription and protein synthesis, and the IRE1 pathway works as an inducer of ER-associated degradation by increasing *XBP1* mRNA splicing. Therefore, it is suggested that T652P inhibits the synthesis of mutated proteins and translocates them from the ER, thereby inducing apoptosis. With the other mutations, only the apoptosis-associated pathway is involved, mainly as shown for the activation of *XBP1*.

However, we speculated that activation of the UPR pathway may partially contribute to the phenotype, because

Table 2 Effect of the expression of various GALC mutants on UPR gene expression in COS-7 cells

	Wild	c.635–646delinsCTC	G270D	P302A	D528N	L618S	T652P	c.635–646delinsCTC/T652P	P302A/L618S
CHOP	△*	ND	△*	ND	△*	△*	*	ND	ND
ATF6	ND	ND	ND	ND	ND	ND	ND	ND	ND
GRP78	ND	ND	ND	ND	ND	ND	**	ND	ND
HERPUD1	ND	ND	ND	ND	ND	ND	**	ND	ND
XBP1s	ND	ND	ND	ND	ND	**	**	**	**

mRNA levels of *CHOP*, *ATF6*, *GRP78*, and *HERPUD1* were compared for the expression of each mutant

ND no significant differences

* Significant difference (increase) $p < 0.05$

** Significant difference (increase) $p < 0.01$

△* Significant difference (decrease) $p < 0.05$

the cytotoxicity of psychosine may be the main factor determining the severity of Krabbe disease. Furthermore, the UPR is known to be composed of several branches or arms, involving the three ER stress sensors ATF6, IRE1, and PERK; however, several downstream factors are common to the branches and different branches activate similar targets but stimulate alternative effects, including apoptosis, protein folding, and anti-oxidant activity, etc. Therefore, different activation in different branches might cause similar cellular effects. SFs expressing the L618S mutant of GALC activated only *CHOP*, which suggested that the pathway of translational attenuation via eIF2α and the induction of apoptosis were mainly activated. On the other hand, SFs expressing the c.635–646delinsCTC mutant of GALC, which contains in-frame insertions/deletions, activated *HERPUD1, CHOP*, and *ATF6*, which suggested that the mechanism of cytoplasmic translocation of the mutated GALC proteins were activated in addition to translational attenuation and apoptosis induction. Most GALC proteins with the L618S mutation are trafficked to the lysosomes [26, 27], whereas those with the c.635–646delinsCTC mutation are trafficked ineffectively; therefore, *HERPUD1* may be activated depending on the amount of mutated GALC in the ER, whereas *CHOP* is activated independent of the mutations. The activation pathways observed in the compound-heterozygous GALC mutant may be a combination of that observed for each mutant. Mutated GALC proteins are also partially trafficked to lysosomes and are subsequently processed to have some enzyme activity depending on the mutations. Therefore, an enhancement of the translocation of mutated GALC proteins to the cytoplasm may lead to a decrease in GALC trafficked to the lysosomes, and therefore also a decrease in residual enzyme activity, which may result in more severe phenotypes. It is speculated that the ER chaperon pathway in addition to the ATF6, PERK, and IRE1 pathways may be activated by the expression of GALC with the missense mutation with low residual enzyme activity. In addition the ATF6, PERK, and IRE1 pathways without the ER chaperon pathway may be activated by the expression of GALC with the missense mutation with high residual GALC enzyme activity. In addition, none of the pathways may be activated by expression of GALC with the nonsense mutation owing to nonsense mRNA decay [28].

There are three main limitations in this study; the cell types used, analysis of the polymorphism in patient SFs and in vivo model animals. First, as UPR activation differs in each cell type [29], the results of transfected COS-7 cells may not apply to clinical conditions. The ATF6, IRE1, and PERK pathways are the main pathways of the UPR and are expressed ubiquitously. On the other hand, old astrocyte-specifically induced substance (OASIS) family proteins, which are ER stress sensors, including LUMAN/CREB3, OASIS/CREB3L1, BBF2H7/CREB3L2, CREBH/CREB3L3, and CREB4/AIbZIP/CREB3L4 demonstrate tissue-specific expression [30]. Although we did not analyze these factors in the current study, we speculate that they may have different effects on UPR activation in COS-7 cells and SFs. Second, we did not coexpress proteins with polymorphisms in COS-7 cells. Some polymorphisms change the trafficking efficiency of proteins to the lysosome [7, 26]. Third, we did not analyze in vivo model animals. Second and third limitations require further investigation in the future [31, 32].

Acknowledgements We thank the patients and their families for their participation in this study. We thank K. Tsujimoto (Osaka University) for technical assistance. This work was supported by the Practical Research Project for Rare/Intractable Diseases (15ek0109151h003) from Japan Agency for Medical Research and Development (AMED), and a Health and Labour Sciences Research Grants (H29-nanchitou (nan)-ippan-024) from Ministry of Health, Labour and Welfare.

Compliance with ethical standards

Conflict of interest The authors declare that they have no conflict of interest.

References

1. Suzuki K, Suzuki Y. Globoid cell leucodystrophy (Krabbe's disease): deficiency of galactocerebroside β-galactosidase. Proc Natl Acad Sci USA. 1970;66:302–9.
2. Chen YQ, Rafi MA, de Gala G, Wenger DA. Cloning and expression of cDNA encoding human galactocerebrosidase, the enzyme deficient in globoid cell leukodystrophy. Hum Mol Genet. 1993;2:1841–5.
3. Sakai N, Inui K, Fujii N, Fukushima H, Nishimoto J, Yanagihara I, et al. Krabbe disease: isolation and characterization of a full-length cDNA for human galactocerebrosidase. Biochem Biophys Res Commun. 1994;198:485–91.
4. Nagano S, Yamada T, Shinnoh N, Furuya H, Taniwaki T, Kira J. Expression and processing of recombinant human galactosylceramidase. Clin Chim Acta. 1998;276:53–61.
5. Hossain MA, Otomo T, Saito S, Ohno K, Sakuraba H, Hamada Y, et al. Late-onset Krabbe disease is predominant in Japan and its mutant precursor protein undergoes more effective processing than the infantile-onset form. Gene. 2014;534:144–54.
6. Lee WC, Kang D, Causevic E, Herdt AR, Eckman EA, Eckman CB. Molecular characterization of mutations that cause globoid cell leukodystrophy and pharmacological rescue using small molecule chemical chaperones. J Neurosci. 2010;30:5489–97.
7. Spratley SJ, Hill CH, Viuff AH, Edgar JR, Skjødt K, Deane JE. Molecular mechanisms of disease pathogenesis differ in Krabbe disease variants. Traffic. 2016;17:908–22.
8. Nagara H, Ogawa H, Sato Y, Kobayashi T, Suzuki K. The twitcher mouse: degeneration of oligodendrocytes in vitro. Brain Res. 1986;391:79–84.
9. Tanaka K, Nagara H, Kobayashi T, Goto I. The twitcher mouse: accumulation of galactosylsphingosine and pathology of the sciatic nerve. Brain Res. 1988;454:340–6.
10. Suzuki K. Twenty five years of the "psychosine hypothesis": a personal perspective of its history and present status. Neurochem Res. 1998;23:251–9.
11. Kaufman RJ. Stress signaling from the lumen of the endoplasmic reticulum: coordination of gene transcriptional and translational controls. Genes Dev. 1999;13:1211–33.
12. Rutkowski DT, Kaufman RJ. A trip to the ER: coping with stress. Trends Cell Biol. 2004;14:20–8.
13. Schröder M, Kaufman RJ. The mammalian unfolded protein response. Annu Rev Biochem. 2005;74:739–89.
14. Shi Y, Vattem KM, Sood R, An J, Liang J, Stramm L, Wek RC. Identification and characterization of pancreatic eukaryotic initiation factor 2 α-subunit kinase, PEK, involved in translational control. Mol Cell Biol. 1998;18:7499–509.
15. Harding HP, Zhang Y, Ron D. Protein translation and folding are coupled by an endoplasmic-reticulum-resident kinase. Nature. 1999;397:271–4.
16. Wei H, Kim SJ, Zhang Z, Tsai PC, Wisniewski KE, Mukherjee AB. ER and oxidative stresses are common mediators of apoptosis in both neurodegenerative and non-neurodegenerative lysosomal storage disorders and are alleviated by chemical chaperones. Hum Mol Genet. 2008;17:469–77.
17. Tessitore A, del P Martin M, Sano R, Ma Y, Mann L, Ingrassia A, et al. GM1-ganglioside-mediated activation of the unfolded protein response causes neuronal death in a neurodegenerative gangliosidosis. Mol Cell. 2004;15:753–66.
18. Zhang Z, Lee YC, Kim SJ, Choi MS, Tsai PC, Xu Y, et al. Palmitoyl-protein thioesterase-1 deficiency mediates the activation of the unfolded protein response and neuronal apoptosis in INCL. Hum Mol Genet. 2006;15:337–46.
19. Villani GR, Chierchia A, Di Napoli D, Di Natale P. Unfolded protein response is not activated in the mucopolysaccharidoses but protein disulfide isomerase 5 is deregulated. J Inherit Metab Dis. 2012;35:479–93.
20. Suzuki T, Shimoda M, Ito K, Hanai S, Aizawa H, Kato T, et al. Expression of human Gaucher disease gene GBA generates neurodevelopmental defects and ER stress in *Drosophila* eye. PLoS ONE. 2006;8:e69147 https://doi.org/10.1371/journal.pone.0069147
21. Sakai N, Fukushima H, Inui K, Fu L, Nishigaki T, Yanagihara I, et al. Human galactocerebrosidase gene: promoter analysis of the 5'-flanking region and structural organization. Biochim Biophys Acta. 1998;1395:62–7.
22. Wenger DA, Rafi MA, Luzi P, Datto J, Costantino-Ceccarini E. Krabbe disease: genetic aspects and progress toward therapy. Mol Genet Metab. 2000;70:1–9.
23. Xu C, Sakai N, Taniike M, Inui K, Ozono K. Six novel mutations detected in the GALC gene in 17 Japanese patients with Krabbe disease, and new genotype-phenotype correlation. J Hum Genet. 2006;51:548–54.
24. Wiederschain G, Raghavan S, Kolodny E. Characterization of 6-hexadecanoylamino4-methylumbelliferyl-β-D-galactopyranoside as fluorogenic substrate of galactocerebrocidase for the diagnosis of Krabbe disease. Clin. Chim. Acta. 1992;205:87–96.
25. Zhong W, Chen X, Jiang P, Wan JM, Qin P, Yu AC. Induction of endoplasmic reticulum stress by sonoporation: linkage to mitochondria-mediated apoptosis initiation. Ultrasound Med Biol. 2013;39:2382–92.
26. Shin D, Feltri ML, Wrabetz L. Altered Trafficking and processing of GALC mutants correlates with globoid cell leukodystrophy severity. J Neurosci. 2016;10:1858–70.
27. Hossain MA, Higaki K, Saito S, Ohno K, Sakuraba H, Nanba E, et al. Chaperon therapy for Krabbe disease: potential for late-onset GALC mutations. J Hum Genet. 2015;60:539–45.
28. Lee WC, Tsoi YK, Dickey CA, Delucia MW, Dickson DW, Eckman CB. Suppression of galactosylceramidase (GALC) expression in the twitcher mouse model of globoid cell leukodystrophy (GLD) is caused by nonsense-mediated mRNA decay (NMD). Neurobiol Dis. 2006;23:273–80.
29. Becker FT, Vitner E, Dekel H, Leshem N, Enquist BI, Karlsson S, et al. No evidence for activation of the unfolded protein response in neuronopathic models of Gaucher disease. Hum Mol Genet. 2009;18:1482–88.
30. Kondo S, Murakami T, Tatsumi K, Ogata M, Kanemoto S, Otori K, et al. OASIS, a CREB/ATF-family member, modulates UPR signalling in astrocytes. Nat Cell Biol. 2005;7:186–94.
31. Kim DY, Kim HR, Kim KK, Park JW, Lee BJ. NELL2 function in the protection of cells against endoplasmic reticulum stress. Mol Cells. 2015;38:145–50.
32. Daffu G, Sohi J, Kamholz J. Proteolipid protein dimerization at cysteine 108: Implications for protein structure. Neurosci Res. 2012;74:144–55.